

Chapter 4

Converter Stability Analysis

4.1 Introduction

Voltage Source Converter (VSC) has been widely used in industrial, commercial and renewable power generation applications. Out of many possible configurations, 3-phase, 3-wire is widely used. During the last decade the penetration of renewable energy sources has increased around the world. This is due to the increased concern worldwide about the carbon emission [336], [337]. The utilization of energy from uncertain and variable sources has become possible with the use of these converters only.

For the purpose of study, analysis of VSC is carried out assuming the ideal operating conditions of grid. But VSCs are never operating under such conditions in practical. In relatively weak system, VSCs are subjected to various power quality disturbances, such as unbalance voltage, voltage swell and sag, notches etc [338]. The occurrence of such disturbances causes various problems like ripples in torque of generator and motor, increased losses, abnormal tripping of protective devices, malfunction of sophisticated control system, reduction in the expected life time of equipment etc [339].

There are two type of harmonics generated by VSCs. One is characteristic harmonics, which are related to the switching frequency of the IGBTs inside the VSC. Another is, non-characteristics harmonics. The voltage ripple on the DC side of VSC generates harmonics on its AC side current. According to [122], the non-characteristics harmonics are generated by the unbalanced voltage on the AC side. However the quantification of the

magnitude of such harmonic is not simple and cannot be done with deterministic method. The non-characteristic harmonics are considered as the steady state low frequency components, which would not appear, if the grid voltage is balanced. The unbalance grid voltage has fundamental frequency negative sequence components and third order positive sequence component.

Though, it is possible to eliminate zero sequence third harmonic component using transformer of the proper vector group. But, the non-characteristic third order positive sequence harmonics cannot be eliminated with transformers having Delta connected winding. In reference [125], the author has proposed DC voltage control to eliminate DC oscillating voltage, when AC side is unbalanced. To achieve this, VSC has to operate with constant AC power control. However, the effect of control on AC current is not discussed. It is important to analyse the distorted and unbalanced AC side current, when such control is implemented. In this case, the currents of AC side of converter contain non-characteristics low frequency component such as fundamental negative sequence and third harmonic component.

In this chapter, the analysis of output impedance of converter with different output filters and different controller topologies have been given.

4.2 Modelling Of Voltage Source Converter

The DC current I_{dc} is flowing to the DC side of VSC. V_{dc} is the instantaneous voltage across the capacitor and i_{dc} is the instantaneous DC current. The Quality Factor of DC capacitor is assumed high, so the series resistance is neglected. The instantaneous active power is supplied by the renewable energy, i.e. Wind Turbine, source to the grid. The instantaneous current I_s is supplied by the external source. It is equal to zero, when VSC operates as a reactive power compensator. The block diagram of VSC control structure is depicted in the figure 4.1. The control system consists of (i) Voltage Control (ii) a Phase Lock Loop (PLL) (iii) Current Reference Calculation block (iv) Current Control. The real power reference is calculated by the PI controller, which considers the DC voltage and desired active power through the VSC to the grid. The instantaneous reactive power is calculated by the separate loop, which may consider either the desired power factor or the

reference voltage. The $d-q$ frame is synchronised with the positive sequence fundamental voltage of the grid at PCC with the help of PLL. It converts three phase voltages V_a, V_b, V_c in to V_d^+ and V_q^+ . Which are converted in the alpha-beta reference frame voltages V_α and V_β . Then current reference is obtained by the $\alpha - \beta$ to $a - b - c$ transformation. These reference currents are compared with actual current and modulating signal m_d and m_q are generated. These signals are finally transformed into m_a, m_b, m_c to generate Pulse Width Modulated (PWM) signal. Both Switching Frequency and Grid Voltage distortion can cause poor power quality. A filter design is a subject requires trade of between filter performance and the control bandwidth. Filters are required to meet power quality standard, avoid parallel resonance and improve power quality. Inverter for grid interfacing will need to incorporate interface filters to attenuate the injection of current harmonics

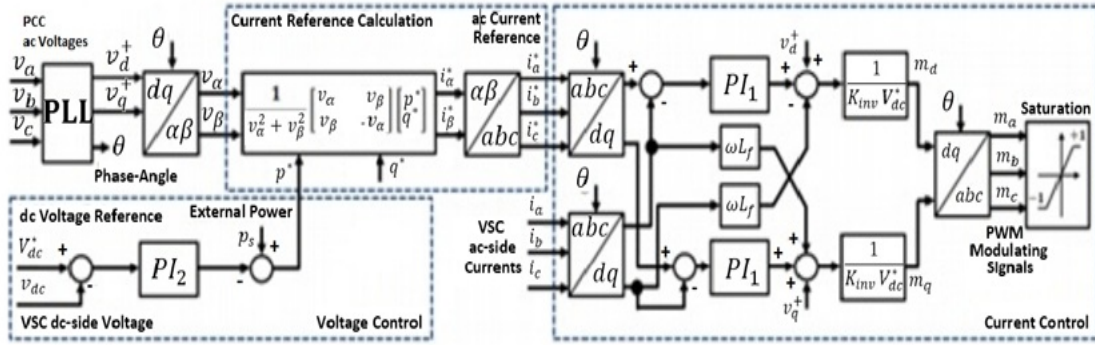


Figure 4.1: Control Structure of Grid Connected Wind Converters

4.3 Impedance Based Stability Analysis

This method was proposed in [8]. The system impedance is partitioned into source and grid impedance. The source impedance is either represented by Thevenins Equivalent circuit or Norton Equivalent circuit. In Thevenins equivalent circuit consists of ideal voltage source in series with the series impedance (Z_s). Whereas the load impedance is modelled by series impedance (Z_l). Since the converter circuit is non-linear, it is represented by the small signal circuit. This linear representation of circuit is valid only for the small perturbation of signal only. With this assumption, the current (I) flowing from source to load is given by

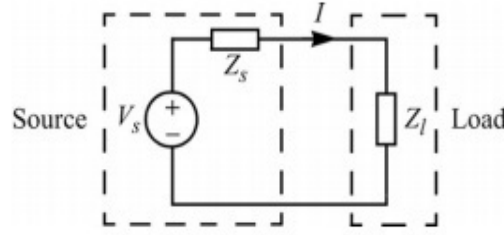


Figure 4.2: Thevenins Equivalent Circuit

$$I_s = \frac{V_s}{Z_l(s) + Z_s(s)} \quad (4.1)$$

Which can be rearranged as,

$$I_s = \frac{V_s}{Z_l(s)} \frac{1}{1 + \frac{Z_s(s)}{Z_l(s)}} \quad (4.2)$$

System Stability analysis is based on the assumption that, the source voltage and load impedance remain stable, i.e. $V(s)$ and $1/Z(s)$ are stable. So, the stability depends on the extreme right hand side of equation (4.2). It is given by

$$H(s) = \frac{1}{1 + \frac{Z_s(s)}{Z_l(s)}} \quad (4.3)$$

The close observation of equation (4.3)) reveals the important characteristics. It is a transfer function with unity gain and feedback equal to $Z_s(s)/Z_l(s)$. According to the linear control theory, the $H(s)$ is stable, if and if only, when ration $Z_s(s)/Z_l(s)$ meets the requirement of Nyquist Stability criterion [8]. In the above analysis for stability, it is assumed that the source is ideal voltage source and it remains stable under unloaded condition. However, the grid connected inverters are usually current controlled. Hence above analysis is not much useful. So, the source should be represented as a current source. To arrive at the equivalent current source, the same small signal voltage source is modified. The voltage across load is given by

$$V(s) = \frac{I_s(s)}{Y_l(s) + Y_h(s)} \quad (4.4)$$

By rearranging equation (4.4),

$$V(s) = \frac{I_s(s)}{Y_l(s)} \frac{1}{1 + \frac{Y_h(s)}{Y_l(s)}} \quad (4.5)$$

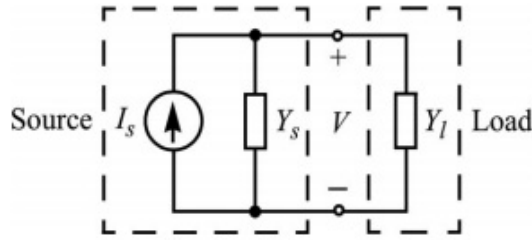


Figure 4.3: Norton's Equivalent Circuit

Similar to the above analysis, the current source is assumed to be stable under unloaded condition. The load is stable when connected to ideal current source. Under this condition of $I(s)$ and $1/Y_l(s)$ are stable. Under this condition, stability of $V(s)$ depends on stability of second term of equation (4.5). This again resembles the closed loop transfer function with negative feedback. The gain is unity and the feedback factor is $Y_s(s)/Y_l(s)$. Therefore the system is stable, if along with above conditions, it meets the Nyquist criterion. In equation (4.5) admittances are used instead of impedance. Though, the analysis still can be carried out in terms of the impedances. In this case equation (4.5) becomes,

$$V(s) = I_s(s)Z_l(s) \frac{1}{1 + \frac{Z_l(s)}{Z_s(s)}} \quad (4.6)$$

It is important to note the requirement of stability. In the voltage source model, the output impedance of source should be as low as possible (ideally zero), whereas in the current source model, the output impedance should be as high as possible (ideally infinite)

4.4 Grid Connected Inverter

The modelling of Impedance of grid connected VSC has a very important use in analysis of stability and resonance phenomena when converter is integrated into the grid [122].

Grid connected converter used in renewable sources is modelled as a current source in parallel with an impedance i.e. Nortons equivalent circuit [122]. The stability of grid connected inverter can be determined by Nyquist criterion [340]. The control structure of most of the VSC is developed in the rotating $d-q$ reference frame [164]. The Phase Lock Loop (PLL) is used to synchronize converter with grid [341]. The use of complex multiple loop control structure introduces non-linearities. These are generally overlooked in the simplified low order modelling [342]. On the flip side, the detailed model introduces complexity and cross-couplings between various terms, which makes the determination of output impedance cumbersome. The trade-off way suggested in some literatures to linearize the model by small signal analysis technique.

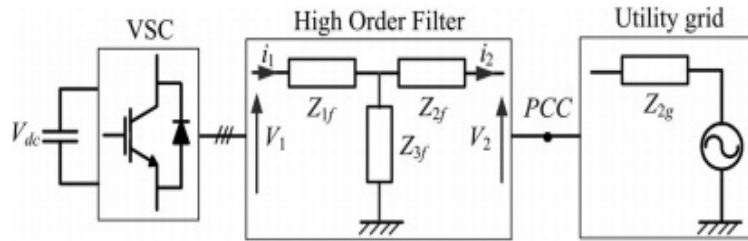


Figure 4.4: Converter Output Circuit

The impedance of Converter interconnected Generator is affected by various factors such as control parameters, PLL, switching delays and converter harmonic filters. The converter is basically controlled by output current signal. In above figure (4.4), i_1 is the converter current and i_2 is grid current. The converter is controlled either by i_1 or i_2 or by difference ($i_1 - i_2$). If the grid current is the control variable, then the current control loop is given by,

$$Y_o(s) = G_{PI}(s)G_D(s)Y_{21}(s) \quad (4.7)$$

Where, Y_{21} is the forward trans-admittance of the filter. G_{PI} is Proportional Integral type current controller and $G_D(s)$ is the switching delay. Here, the converter output voltage is considered as pure sinusoidal, if there is a noise in the voltage, then it needs to be considered as a disturbance signal. If, the converter is controlled by taking converter current i_1 then Y_{21} is replaced by output conductance Y_{11} . The forward trans-conductance Y_{21} is given by,

$$Y_{21}(s) = \frac{Z_{3f}}{Z_{1f}Z_{2f} + Z_{2f}Z_{3f} + Z_{1f}Z_{3f}} \quad (4.8)$$

The simple transfer function of PI type current controller is given by,

$$G_{PI} = k_p + \frac{k_i}{s} \quad (4.9)$$

Higher order controller also can be used for current control, but here simple PI controller is considered for sake of simplicity. The delay has been approximated by Pades approximation technique. It is expressed mathematically as,

$$G_D(s) = \frac{1}{1 + 1.5T_d s} \quad (4.10)$$

The frequency response of output impedance can be plotted with different short circuit level (i.e grid strength) of the grid to check the stability by observing Gain Margin (GM) and Phase Margin (PM). The phase at the zero gain gives the Phase Margin (PM) and gain at phase angle of 180° gives the Gain Margin (GM).

4.5 Phase Lock Loop (PLL)

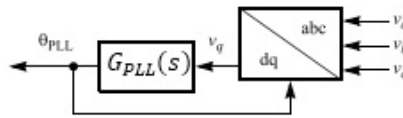


Figure 4.5: Phase Lock Loop (PLL)

The Phase Lock Loop (PLL) is basically a PI controller. So, the structure of PLL should be thoroughly assessed for stability assessment. Proper structure of PLL and control scheme helps to mitigate adverse impact on the system. The purpose of PLL is to synchronize converter with grid. Harmonics in the grid may penetrate to converter through PI controller. If, control parameters are not properly chosen, this may produce harmonics through circular effect. Figure (4.5) shows the block diagram of PLL . The detail block diagram is given in figure (4.6).

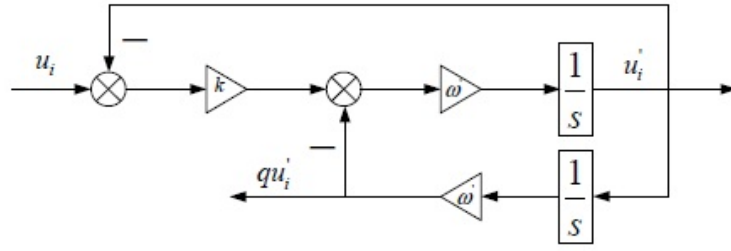


Figure 4.6: Block Diagram of Simple Phase Lock Loop

$$G_{PLL}(s) = f(s, w, k) \quad (4.11)$$

Figure (4.6) is the traditional Second Order Generalized Integrator Quadrature Signal Generator (SOGI – QSG) PLL. This can filter out higher order harmonics. Where u_i is the input signal and u_i' , qu_i' are two output signal, which are in quadrature. k is the damping coefficient and ω is the output angular frequency of PLL. Equations (4.14) and (4.15) shows the transfer function of PLL.

$$G_1(s) = \frac{u_i'}{u_i} \quad (4.12)$$

$$u_i' = [(u_i - u_i')k - u_i' \frac{\omega'}{s}] \times \frac{\omega'}{s} \quad (4.13)$$

The inphase gain $G_1(s)$ is given by,

$$G_1(s) = \frac{u_i'}{u_i} = \frac{k\omega' s}{s^2 + k\omega' s + \omega'^2} \quad (4.14)$$

Similarly, quadrature output transfer function is,

$$H(s) = \frac{qu_i'}{u_i} = \frac{k\omega'^2}{s^2 + k\omega' s + \omega'^2} \quad (4.15)$$

In traditional SOGI-QSG PLL, the DC component in the input signal is not suppressed by the PLL. To overcome this problem, a minor modification is made in above PLL. The modified PLL is shown in figure (4.7).

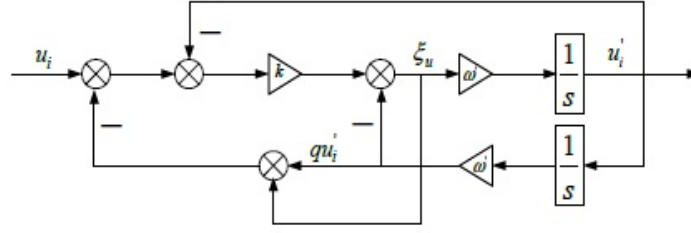


Figure 4.7: Block Diagram of Modified Phase Lock Loop

Transfer functions of modified PLL is given by equations (4.16), (4.17) and (4.18). This structure reduces the tracking error of PLL.

$$F_2(s) = \frac{\xi'_u}{u_i} = \frac{ks^2}{s^2 + k\omega's + \omega'^2} \quad (4.16)$$

$$G_2(s) = \frac{u'_i}{u_i} = \frac{k\omega's}{(k+1)s^2 + k\omega's + (k+1)\omega'^2} \quad (4.17)$$

$$G_2(s) = \frac{qu'_i}{u_i} = \frac{k\omega'^2}{(k+1)s^2 + k\omega's + (k+1)\omega'^2} \quad (4.18)$$

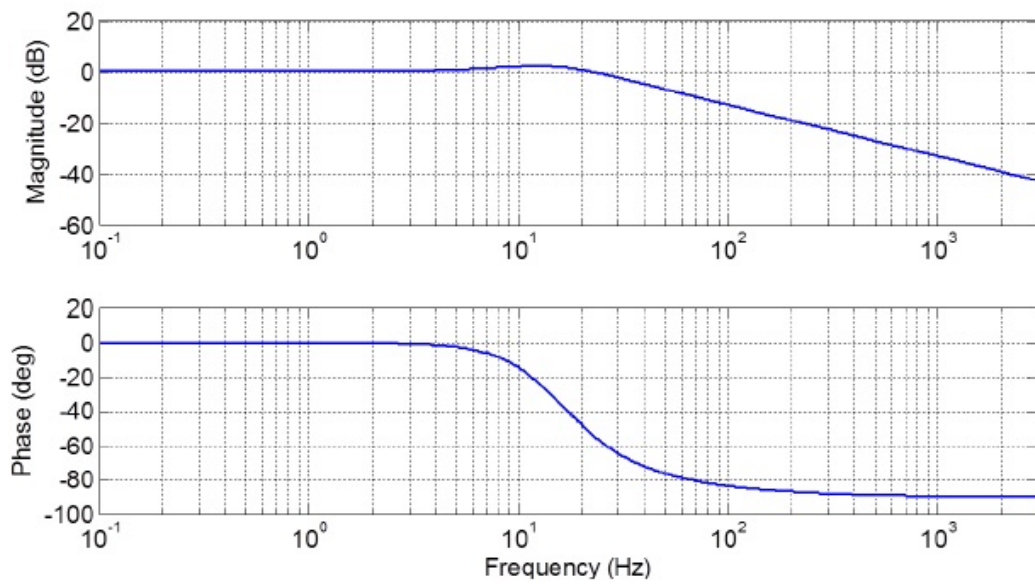
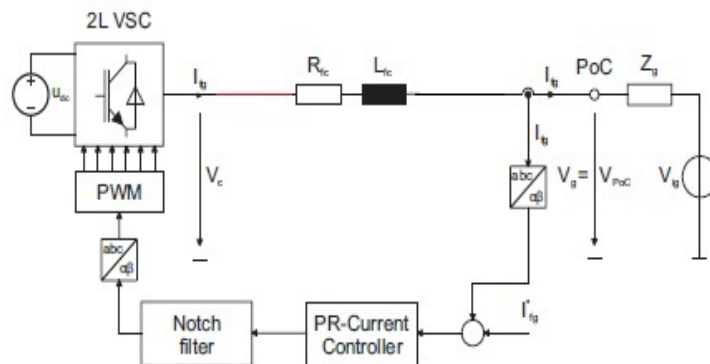


Figure 4.8: Frequency Response of Simple Phase Lock Loop

4.6 Damped Passive Filter Topologies

4.6.1 R-L Filter



Applying KVL at the converter output gives,

Converter output is controlled by output current,

$$V_c = f(I_{fq}) \quad (4.20)$$

With simple PI controller, the output becomes,

$$V_c = (k_p + \frac{k_i}{s})(I_{fg}) \quad (4.21)$$

Putting equation (4.21) into equation (4.19),

$$(k_p + \frac{k_i}{s})(I_{fg}) - V_{POC} = I_{fg}(R_{fc} + sL_{fc}) \quad (4.22)$$

$$(k_p + \frac{k_i}{s})(I_{fg}) - I_{fg}(R_{fc} + sL_{fc}) = V_{POC} \quad (4.23)$$

$$Z_o = \frac{(s^2L_{fc} + s(R_{fc} - k_p) - k_i)}{s} \quad (4.24)$$

$$Z_o = \frac{(s + \alpha)(s + \beta)}{s} \quad (4.25)$$

Considering $(\alpha < \beta)$.

The above equation (4.25) shows that, there are two zeros and one pole. First, the output impedance decreases at -20 dB per decade up to first zero at α . At α , the impedance response becomes flat and at β the impedance starts increasing at 20 dB per decade. So, the response of an integrated filter becomes similar to that of series resonance filter. The selection of α & β depends on the parameter selection of L_{fc} , R_{fc} , k_p and k_i . Bode plot for R-L filter without and with the *PI* current controller has been given in figure (4.10) and (4.11) respectively. The value of resistance R_{fc} varies for fixed value of other parameters ($L_{fc} = 4mH$, $k_p = 1.2$ and $k_i = 11.6$).

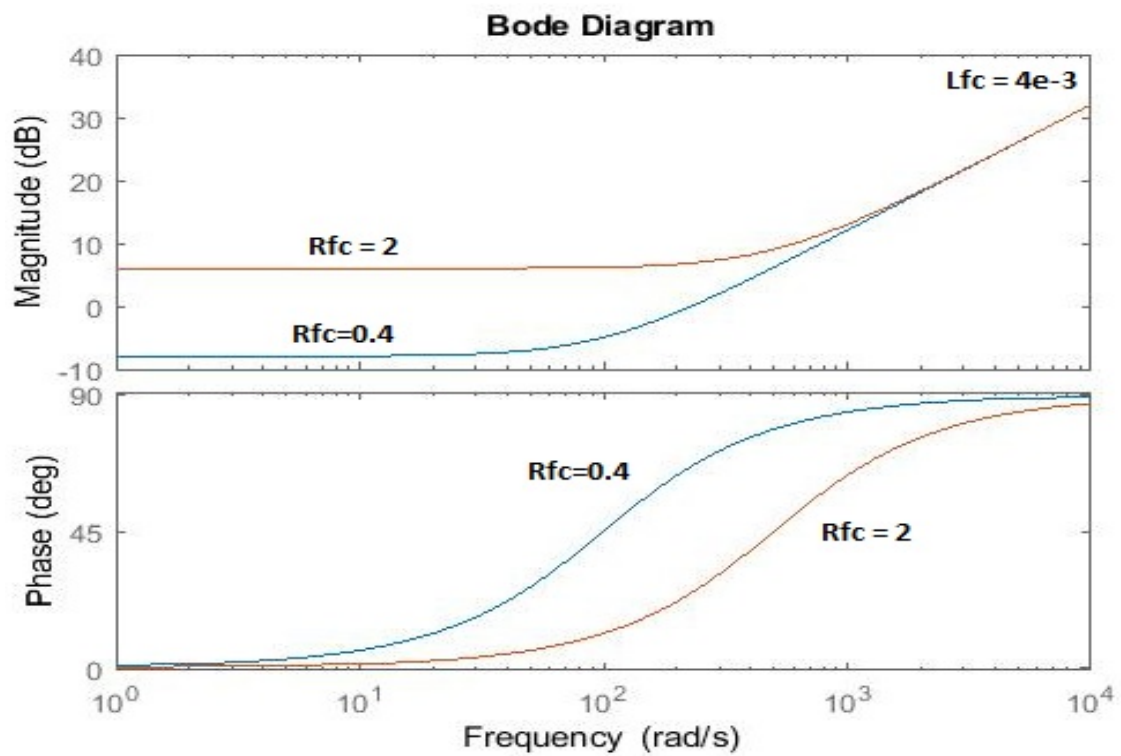


Figure 4.10: Frequency Response of Impedance with RL Filter without PI Controller

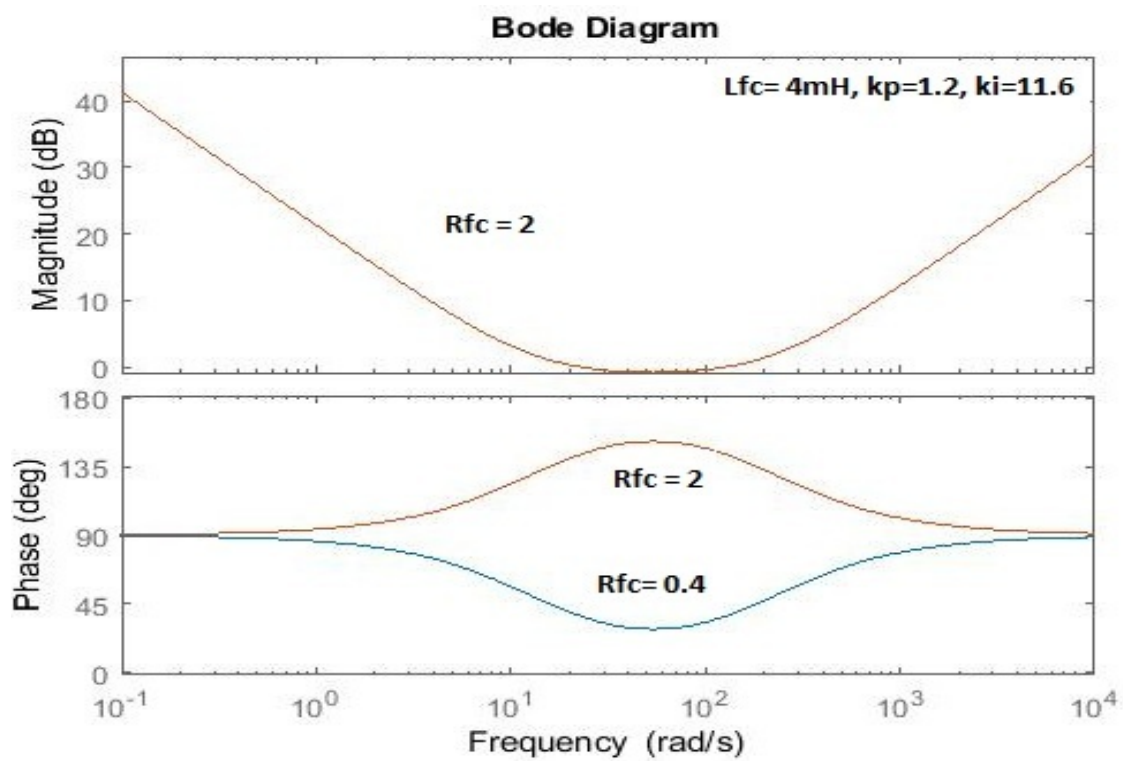


Figure 4.11: Frequency Response of Impedance with RL Filter with PI Controller

Now, the analysis is done with inclusion of PI controller. From figure (4.11), it can be inferred that as the filter resistance decreases, Phase Margin PM improves. The Quality Factor of R-L filter plays important in the stability of converter.

4.6.2 L-C Filter

L-C filter is used in converters for industrial applications like a Variable Frequency Drive (VFD) and Uninterrupted Power Supply (UPS). It is simple in construction and relatively less costly. The analysis of L-C filter with PI controller is given here.

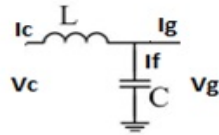


Figure 4.12: L-C Filter

As per the standard practice, the value of L is selected such that its impedance at fundamental frequency should not drop voltage more than 3% of rated voltage. The capacitive reactance offers $1/5^{th}$ of the fundamental inductive reactance at the switching frequency of converter (around 3 - 4 kHz) to absorb harmonics effectively. Based on these criteria $L - C$ filter has been designed widely. The frequency response of $L - C$ filter with and without PI controller is given in figure (4.13) and (4.14) respectively. It is clear from the difference in bode plot that PI controller changes the frequency response. The filter parameters are $L = 4mH$ and $C = 5\mu F$. The inherent resistance of the capacitor and inductor has been neglected.

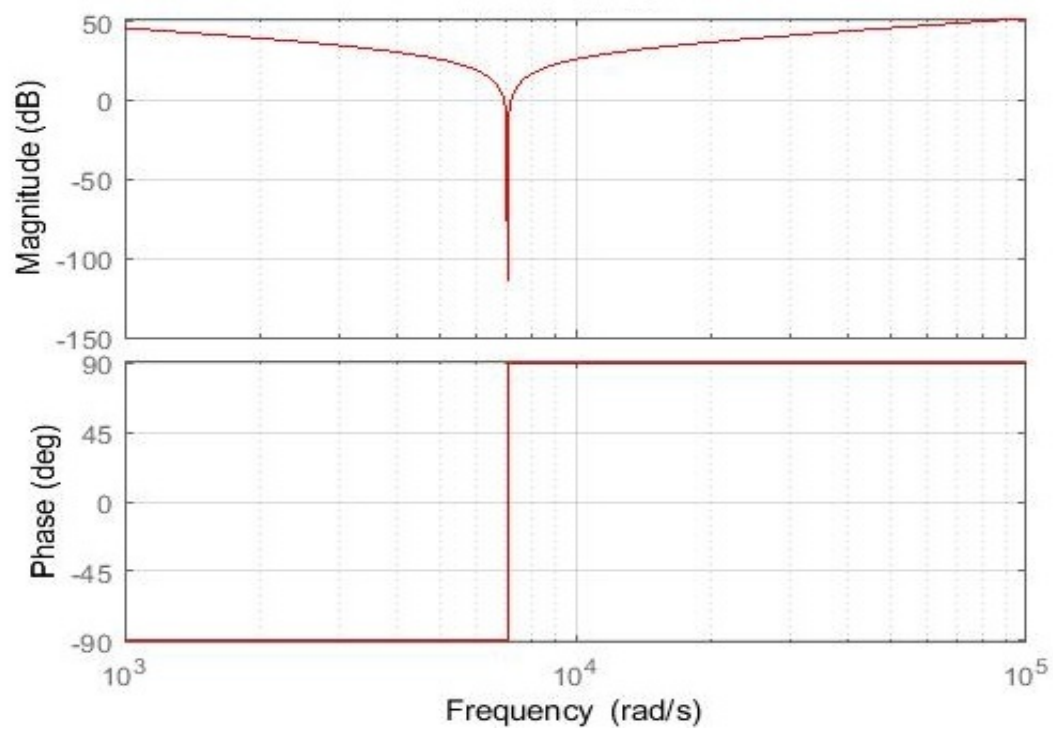
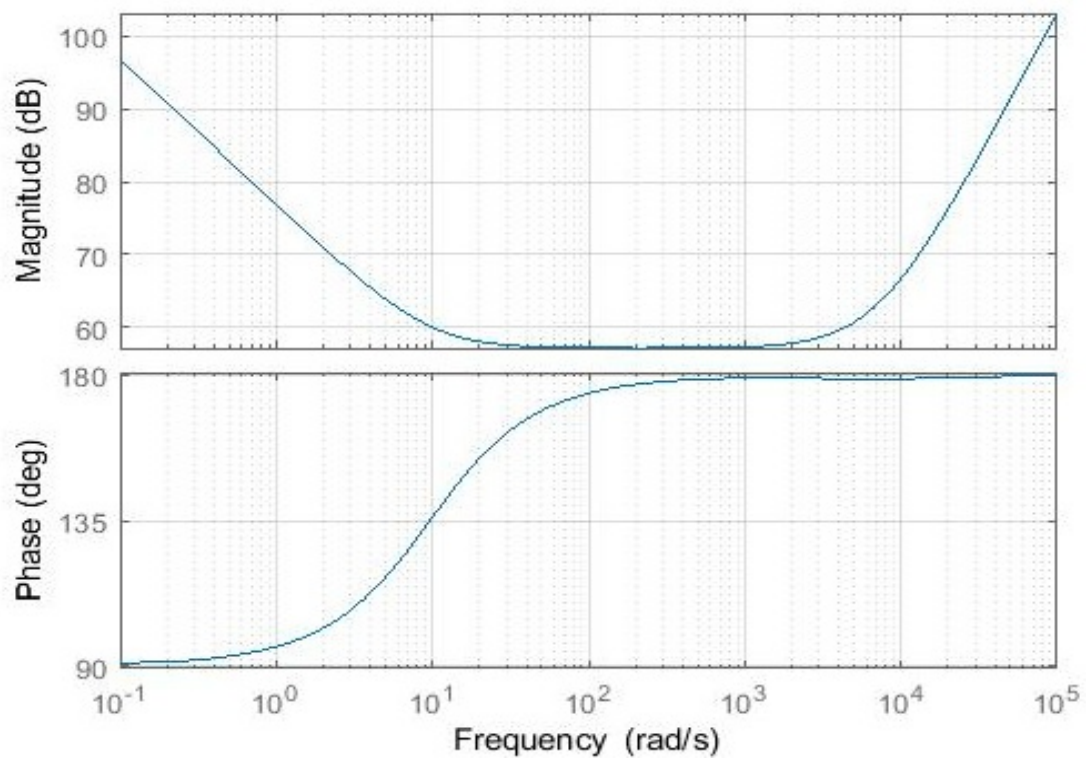


Figure 4.13: Frequency Response of LC Filter without PI Controller

Figure 4.14: Frequency Response of LC Filter with *PI* Controller

It is apparent from figure (4.13) and (4.14) that, the frequency response of L-C filter is completely changed by the action of *PI* controller. The value of *PI* controller parameter k_p and k_i decides the Gain Margin (*GM*), Phase (*PM*), Gain Margin Cut Off frequency (ω_{cg}) and Phase Margin Cut Off frequency (ω_{cp}). Here $k_p = 1.2$ and $k_i = 11.6$ is selected for analysis purpose for $L = 4mH$ and $C = 5\mu F$.

4.6.3 L-C-L Filter

Initially, L-C filter was used for converter applications, but grid connected inverter has unique requirements that L-C filter may not fulfil. Properly designed L-C-L filter may overcome the drawbacks of L-C filter.

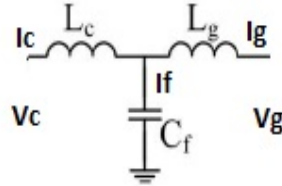


Figure 4.15: L-C-L Filter

Applying KVL,

$$V_c = \left(\frac{(V_g + L_g s I_g)}{1/sC_f + R} + I_g \right) sL_c \quad (4.26)$$

The converter output voltage V_c is a function of the grid current I_g . Then,

$$V_c = f(I_g) \quad (4.27)$$

$$V_c = \left(k_p + \frac{k_i}{s} \right) I_g \quad (4.28)$$

Putting this in equation 4.26 and simplifying further gives,

$$Z_o = \frac{V_g}{(-I_g)} = \frac{a_4 s^4 + a_3 s^3 + a_2 s^2 + a_1 s + a_0}{b_3 s^3 + b_2 s^2 + b_1 s + b_0} \quad (4.29)$$

Where,

$$a_4 = L_g C_f k_p$$

$$a_3 = L_g C_f k_i + R C_f L_g k_p$$

$$a_2 = R L_g C_f k_i + L_c k_p - C_f$$

$$a_1 = L_c k_i$$

$$a_0 = 0$$

$$b_3 = L_c C_f k_p$$

$$b_2 = L_c C_f k_i$$

$$b_1 = 0$$

$$b_0 = 0$$

$$L_c = 4mH, L_g = 0.4mH, C_f = 5\mu F, k_p = 1.2, k_i = 11.6$$

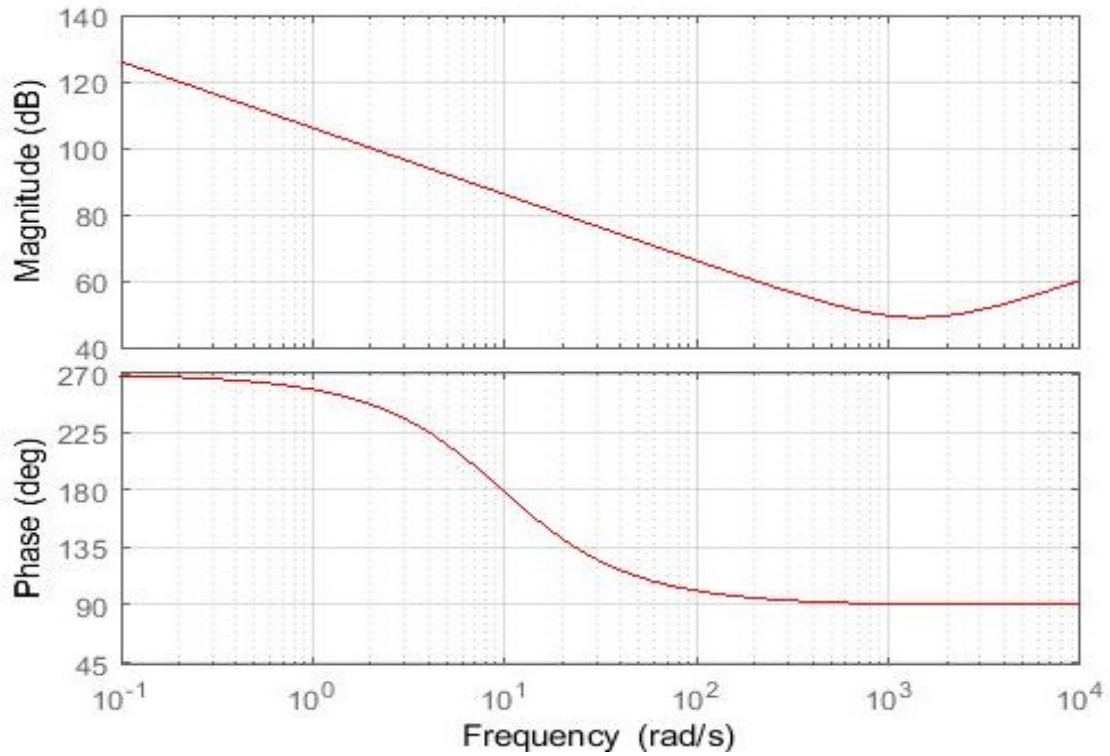


Figure 4.16: Frequency Response of L-C-L Filter with PI Controller

The figure (4.16) shows the frequency response of L-C-L filter together with PI controller. It is clear from equation (4.29) and from the figure (4.16), the PI controller increases the order of filter, so the frequency response of passive filter gets changed by the controller action.

4.7 L-C-L Filter Design

The design criterion for filter design should comply with the regulatory requirement. As per IEEE 519-1992 standard, the current harmonics for weak grid condition (I_{sc}/I_L) should be less than 0.3%. The ripple is caused by Pulse Width Modulated (PWM) signal. Output voltage varies from zero level to DC voltage level (V_{dc}). The modulated wave cause ripples in the current, which can be reduced by proper selection of output filter parameters. Typical L - C - L filter has been used in most of the inverter. The $L_1 - C - L_2$ filter has three unknown. The selection of these parameters depends on various factors. Grid condition is one of them. The strength of the grid decides the effectiveness of filters [343], [344]. Typical grid impedance varies from 5% to 8% with X/R ratio in the range of 7 to 10 [298].

The switching frequency decides the ripple level and ripple frequency. Generally, inverter switching frequency remains in the range of 3 to 5 kHz. The ripple current is reduced either by increasing switching frequency or by using a passive filter at the inverter/converter output. Higher switching frequency is selected to reduce the ripple current at the generation point, but it adversely affects the converter (IGBT) losses [345]. The second option is to use a large inductor at the output of converter, but this not only incur high cost, but also increases the core losses. Typically 20% ripple current is expected in the output current. Keeping this in consideration, the inductor L_1 is given by [346].

$$L_1 = \frac{1}{8} \frac{V_{dc}}{\Delta I_L f_{sw}} = \frac{1}{8} \times \frac{V_{dc}}{0.2 \times I_{rated} \times f_{sw}} \quad (4.30)$$

The capacitor rating is selected such that the reactive power of capacitor is neither too high nor too low. Higher reactive power demands more power from converter, which cause more loss in reactor L_1 and also more loss in converter switches. A lower value of capacitor will increase the inductor size. Keeping this into consideration, the capacitor has been selected so that the reactive power should be in the range of 15% to 20% of the rated power.

$$C_1 = 0.15 \times \frac{P_r}{\omega \times V_r^2} \quad (4.31)$$

There is no specific rule or guideline for value of L_2 . It's value is selected based on the grid strength.

4.8 Results and Discussion

The filter design is critical from stability point of view. The desynchronization of Grid Inverter (Grid Inverter Tripping) has been widely observed in the field due to harmonic resonance. The method of active and passive damping has been discussed in this chapter. The results of active and passive damping are given here.

4.8.1 Passive Damping of Filter

4.8.1.1 Type-I Filter

In L-C-L filter, the damping can be achieved by simply adding series resistance in series with capacitor C. It is obvious that large value of damping resistance (R_d) gives large damping. But, damping is effective around the resonance point only [346]. Above the resonance point damping weakens. Also, the large value of resistance cause higher losses

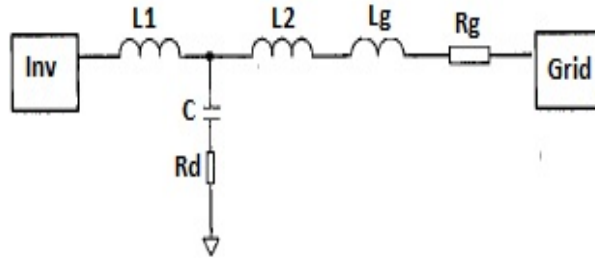


Figure 4.17: Type-I L-C-L Filter

Impedance of Type-I LCL filter with damping resistance is given by,

$$Z_o = \frac{V_g}{(-I_g)} = \frac{a_4 s^4 + a_3 s^3 + a_2 s^2 + a_1 s + a_0}{b_2 s^2 + b_1 s + b_0} \quad (4.32)$$

Where,

$$a_4 = L_g L_1 C^2$$

$$a_3 = L_1 C^2 (R_d + R_g)$$

$$a_2 = L_g R_d C + L_1 C$$

$$a_1 = L_g + C R_d R_g$$

$$a_0 = R_g$$

$$b_2 = L_g C$$

$$b_1 = (R_g + R_d) C$$

$$b_0 = 1$$

$$L_1 = 0.45mH, L_2 = 0.30mH, L_g = 0.212mH, R_g = 0.0095\Omega, C = 270\mu F, R_d = 0.05\Omega - 0.8\Omega$$

Analysis of frequency response of L-C-L filter with damping resistor is given in figure 4.18. The grid parameter are $L_g = 0.212mH$ and $R_g = 0.0095\Omega$, whereas the filter parameters are $L_1 = 0.450mH$, $L_2 = 0.300mH$ and $C = 270\mu F$. The damping resistance R_d is varied from 0.05Ω to 0.8Ω . It is clear from the plot that, the response of impedance is similar to inductive impedance. The notch is observed at the resonance frequency. The notch can be smoothened with higher value of damping resistor R_d . For small value of R_d , a positive spike in gain is observed, which goes to negative with increase in value of R_d . If, R_d is increased further, it dampens out the notch, but system remain marginally stable, as the gain margin decreases to very low value and it can be observed from figuer (4.18). The minimum value of R_d which brings the system into stable region is 1.01Ω . At this value, the gain margin is $\approx -30dB$, and phase margin is 9.23° . The gain margin crossover frequency is 3950 rad/sec and phase margin crossover frequency is 4630 rad/sec . With increase in value of R_d by 0.1Ω reduces the gain margin to $\approx -3dB$ and phase margin to 2.1788° , which is very drastically reduction. So, the value of R_d has to be selected very carefully for this Type-I variant of L-C-L filter.

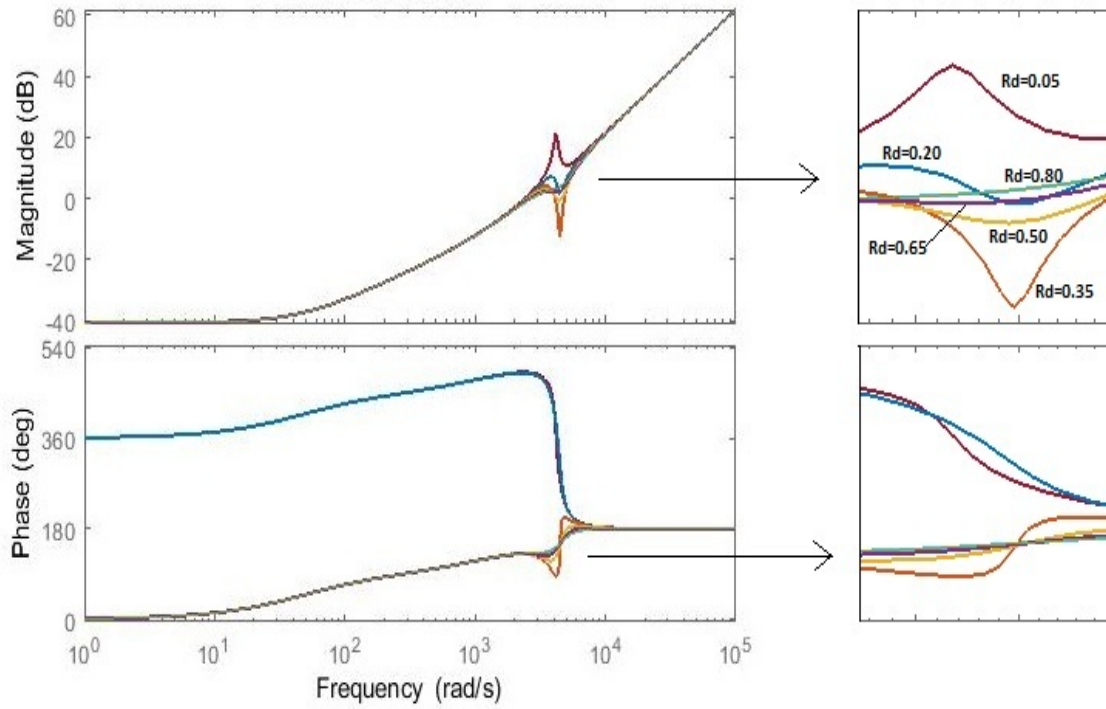


Figure 4.18: Frequency Response of Type-I L-C-L Filter

4.8.1.2 Type-II Filter

In Type-II LCL filter, the damping can be achieved by simply adding a parallel combination of resistor and inductor in series with capacitor C. The effect of inductor is investigated using Bode plot. The inductor L_f has been selected as a damping parameter instead of resistor R_f . The value of R_f is fixed and L_f is varied and the effect on frequency response is observed. The value of $R_f = 10\Omega$ and L_f is varied from $50\mu H$ to $500\mu H$. The effect of increase in L_f is observed using frequency response is given in figure (4.20). At $L_f = 50\mu H$, the gain margin is $109.6dB$ and phase margin is 90.44° . The gain margin crossover frequency is 2567 rad/sec and phase margin crossover frequency is 204.98 rad/sec . At $L_f = 500\mu H$, the gain margin is $85.35dB$ and phase margin is 89.80° . The gain margin crossover frequency is 1912 rad/sec and phase margin crossover frequency is 204.62 rad/sec . So, from this result, it is inferred that the effect of inductor L_f on phase margin and phase margin crossover frequency is not much. However, it affects the gain margin and gain cross over frequency. In fact, it reduces the gain crossover frequency and bringing down near to lower order harmonics. So, it is verified that lower value of

inductor L_f offers better gain margin and higher gain crossover frequency, which is very vital from converter stability point of view.

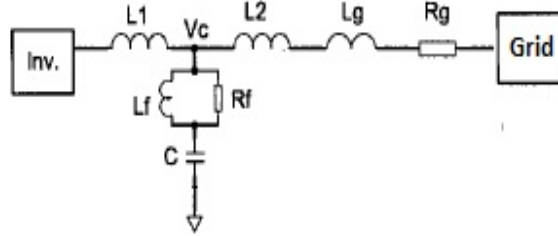


Figure 4.19: Type-II L-C-L Filter

Impedance of Type-II L-C-L filter with damping Inductor and resistance is given by,

$$Z_o = \frac{V_g}{(-I_g)} = \frac{a_4 s^4 + a_3 s^3 + a_2 s^2 + a_1 s + a_0}{b_3 s^3 + b_2 s^2 + b_1 s + b_0} \quad (4.33)$$

Where,

$$a_4 = CL_1 L_f (L_g + L_2)$$

$$a_3 = L_1 CL_f R_f + CL_1 L_f R_g + CR_f (L_2 + L_g) + CR_f L_f (L_2 + L_g)$$

$$a_2 = L_1 L_f + CL_1 R_f R_g + CL_f R_f R_g + L_f (L_2 + L_g)$$

$$a_1 = L_1 R_f + L_f R_g + R_f (L_2 + L_g)$$

$$a_0 = R_f R_g$$

$$b_3 = CL_f (L_2 + L_g)$$

$$b_2 = CL_f R_f + CL_f R_g + CR_f (L_2 + L_g)$$

$$b_1 = L_f + CR_f R_g$$

$$b_0 = R_f$$

$$L_1 = 0.45mH, L_2 = 0.30mH, L_g = 0.212mH, R_g = 0.0095\Omega, C = 270\mu F, R_f = 10\Omega, L_f = 50\mu H - 500\mu H$$

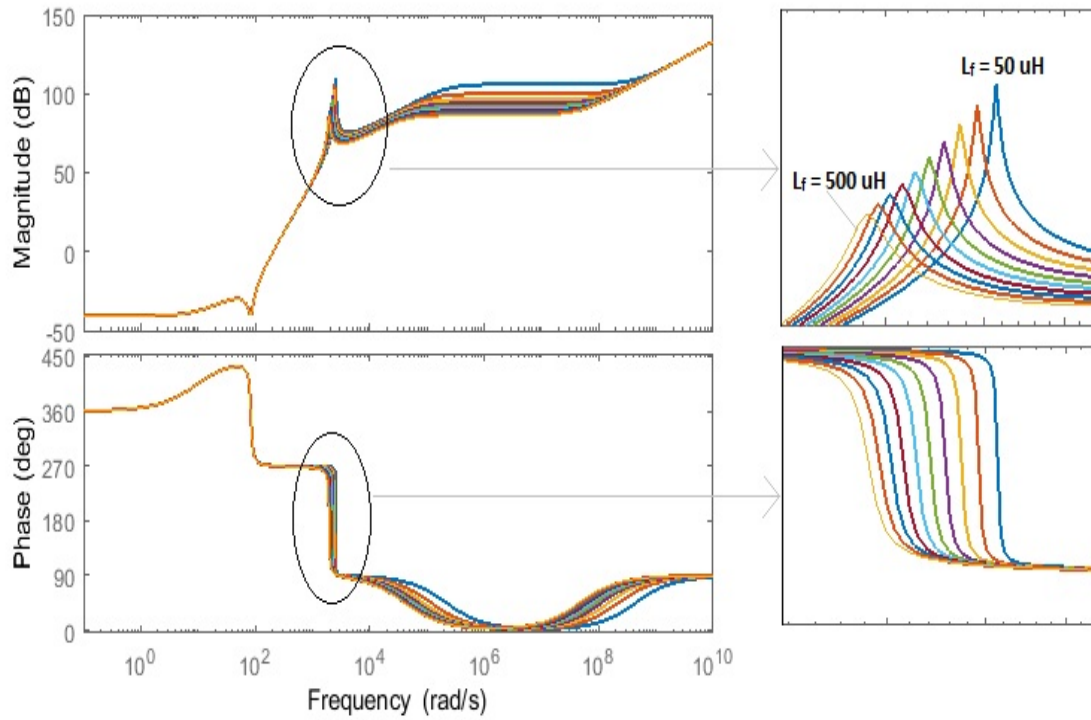


Figure 4.20: Frequency Response of Type-II L-C-L Filter

From the bode graph, it is observed that the gain margin is $70 - 110\text{dB}$ for various values of L_f . Similarly, the phase margin is 90° . As the value of L_f is increased, there will be reduction in the gain margin.

4.8.1.3 Type-III Filter

In Type-III L-C-L filter, the damping can be achieved by simply adding parallel combination of resistor R_f and inductor L_f in series with capacitor C . The effect of inductor is investigated using Bode plot.

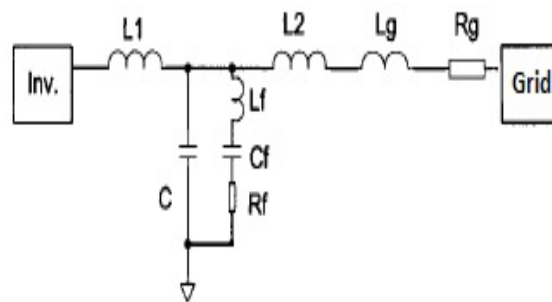


Figure 4.21: Type-III L-C-L Filter

Impedance of Type—III L-C-L filter with damping Inductor and resistance is given by,

$$Z_o = \frac{V_g}{(-I_g)} = \frac{a_4 s^4 + a_3 s^3 + a_2 s^2 + a_1 s^1 + a_0 s^0}{b_3 s^3 + b_2 s^2 + b_1 s^1 + b_0 s^0} \quad (4.34)$$

Where,

$$a_4 = CC_f L_1 (L_g + L_2) + CL_1 L_f C_f$$

$$a_3 = L_1 CC_f R_g + CL_1 C_f R_f + C_f L_f (L_2 + L_g)$$

$$a_2 = L_1 C + C_f (L_2 + L_g) R_f + C_f L_f R_g$$

$$a_1 = L_1 C_f + C_f R_g R_f + (L_2 + L_g)$$

$$a_0 = R_g$$

$$b_3 = CC_f (L_2 + L_g) + CL_f C_f$$

$$b_2 = CC_f R_g + CC_f R_f$$

$$b_1 = C_f$$

$$b_0 = 0$$

$$L_1 = 0.45mH, L_2 = 0.30mH, L_g = 0.212mH, R_g = 0.0095\Omega, C = 270\mu F, C_f = 1\mu F, R_f = 0.5\Omega, L_f = 2.8mH - 28mH$$

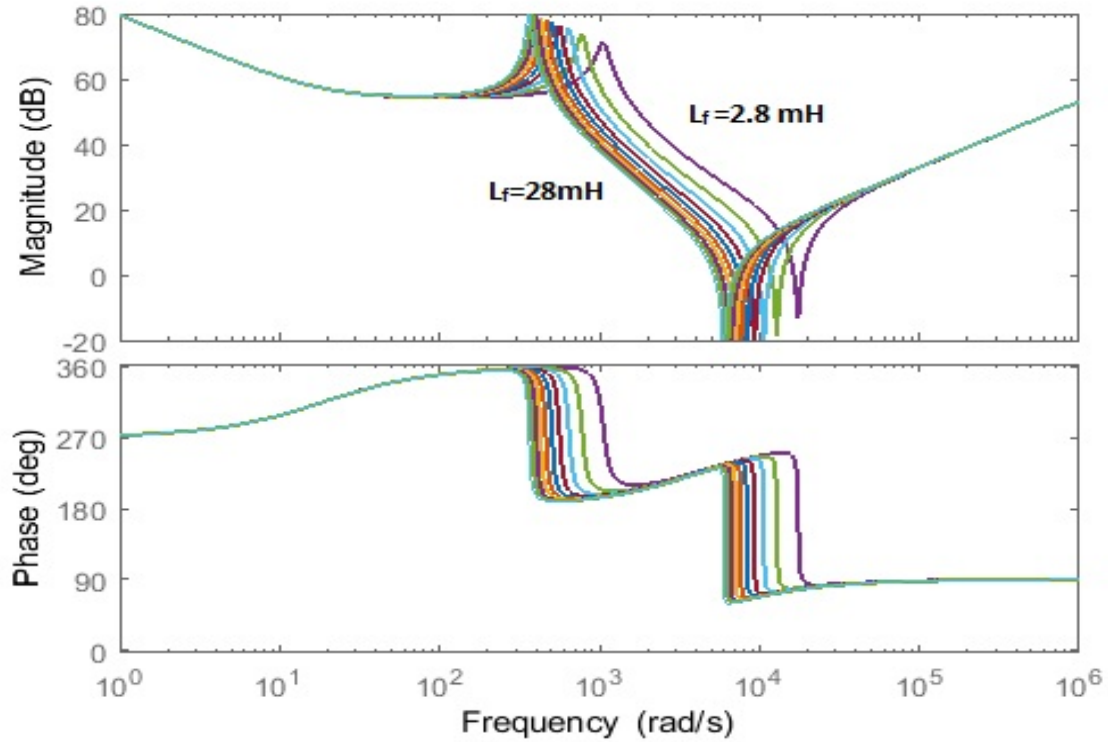


Figure 4.22: Frequency Response of Type—III L-C-L Filter

Impedance shows two resonance points, first is a parallel resonance and second is a series resonance. At first resonance point, the output impedance increases and at series resistance it is at the minimum value. To achieve damping effect, the value of inductor L_f is varied from 2.8 mH to 28 mH for a fixed value of R_f and C_f . For $L_f = 2.8 \text{ mH}$, the gain margin is -13.13dB and phase margin is 63.82° . The gain crossover frequency is 17390 rad/sec and phase cross over frequency is 16434 rad/sec. With $L_f = 28\text{mH}$, the gain margin is -0.44dB and phase margin is 49.85° . The gain cross over frequency is 5928 rad/sec and phase crossover frequency is 5142 rad/sec. So, the higher value of inductor is not suggested as it brings down the gain and phase margin as well as crossover frequencies.

4.8.1.4 Type–IV Filter

In Type–IV L-C-L filter, the damping can be achieved by simply adding parallel combination of resistor with capacitor C_f . The effect of resistor value has been investigated using bode plot. To achieve the impedance reshaping, the value of resistor R_f is varied in the range of 0.5Ω to 5Ω . For $R_f = 0.5 \Omega$, the gain margin is -136.11dB and phase margin is 90° . The gain cross over frequency is 278.38 rad/sec and phase cross over frequency is 34.51 rad/sec.

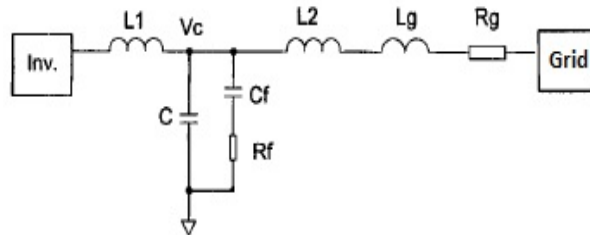


Figure 4.23: Type–IV L-C-L Filter

Impedance of Type–IV L-C-L filter with damping resistor R_f in series with capacitor C_f is given by,

$$Z_o = \frac{V_g}{(-I_g)} = \frac{a_4 s^4 + a_3 s^3 + a_2 s^2 + a_1 s^1 + a_0 s^0}{b_3 s^3 + b_2 s^2 + b_1 s^1 + b_0 s^0} \quad (4.35)$$

Where,

$$a_4 = CC_f L_1 (L_g + L_2)$$

$$a_3 = CC_f L_1 R_f + CC_f L_1 R_g$$

$$a_2 = L_1 C_f + L_1 C + C_f R_f (L_2 + L_g) + C_f (L_2 + L_g)$$

$$a_1 = C_f R_f R_g$$

$$a_0 = R_g$$

$$b_3 = CC_f (L_2 + L_g)$$

$$b_2 = CC_f R_g + CC_f R_f$$

$$b_1 = C_f + C$$

$$b_0 = 0$$

$$L_1 = 0.45mH, L_2 = 0.30mH, L_g = 0.212mH, R_g = 0.0095\Omega, C = 270\mu F, C_f = 1\mu F, R_f = 0.5\Omega - 5\Omega, L_f = 0mH$$

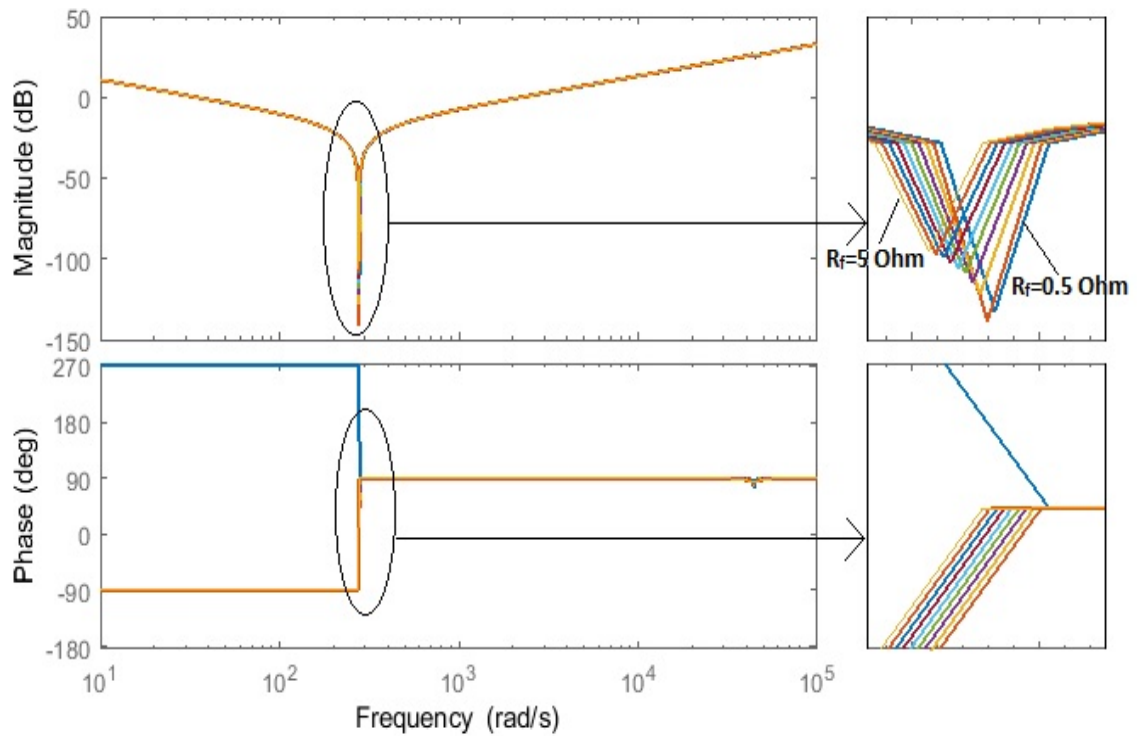


Figure 4.24: Frequency Response of Type-IV L-C-L Filter

The response of Type-IV filter is similar to the tuned filter. The notch in frequency response of impedance is observed at the resonant frequency. This notch can be damped by putting higher value of resistor in series with the capacitor C_f . The phase of impedance

sharply changes from -90° to 90° , It means, the nature of impedance turns from capacitive to inductive. The ratio of C_f/C decides the damping effectiveness. Larger the C_f/C ratio, larger will be the damping. Also, with increasing value of C_f/C ratio, the loss in resistor R_f is also increase as more and more current tends to flow in it [347], [348], [349].

4.8.1.5 Type–V Filter

In Type–V L-C-L filter, the damping can be achieved by simply adding parallel combination of a resistor and an inductor with a capacitor C. The effect of inductor has been investigated using Bode plot.

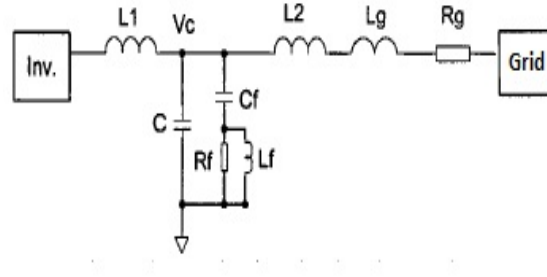


Figure 4.25: Type–V L-C-L Filter

Impedance of Type–V LCL filter is given by,

$$Z_o = \frac{V_g}{(-I_g)} = \frac{a_5 s^5 + a_4 s^4 + a_3 s^3 + a_2 s^2 + a_1 s^1 + a_0 s^0}{b_4 s^4 + b_3 s^3 + b_2 s^2 + b_1 s^1 + b_0 s^0} \quad (4.36)$$

Where,

$$a_5 = CC_f L_1 L_f (L_g + L_2)$$

$$a_4 = CC_f L_1 L_f R_f + CC_f L_1 R_f (L_g + L_2) + CC_f L_1 L_f R_g$$

$$a_3 = CL_f L_1 + CC_f L_1 R_f + C_f L_f R_f (L_g + L_2)$$

$$a_2 = L_1 C R_f + L_f (L_2 + L_g) + L_f C_f R_f R_g$$

$$a_1 = L_1 + R_f (L_2 + L_g) + L_f R_g$$

$$a_0 = R_f R_g$$

$$b_4 = L_f C C_f (L_2 + L_g)$$

$$b_3 = L_f C C_f R_f + L_f C C_f R_g + C C_f R_f (L_2 + L_g)$$

$$b_2 = L_f C + C C_f R_f$$

$$b_1 = R_f C$$

$$b_0 = 1$$

$$L_1 = 0.45 \text{ mH}, L_2 = 0.30 \text{ mH}, L_g = 0.212 \text{ mH}, R_g = 0.0095 \Omega, C = 270 \mu\text{F}, C_f = 1 \mu\text{F}, R_f = 10 \Omega - 100 \Omega, L_f = 2.8 \text{ mH}$$

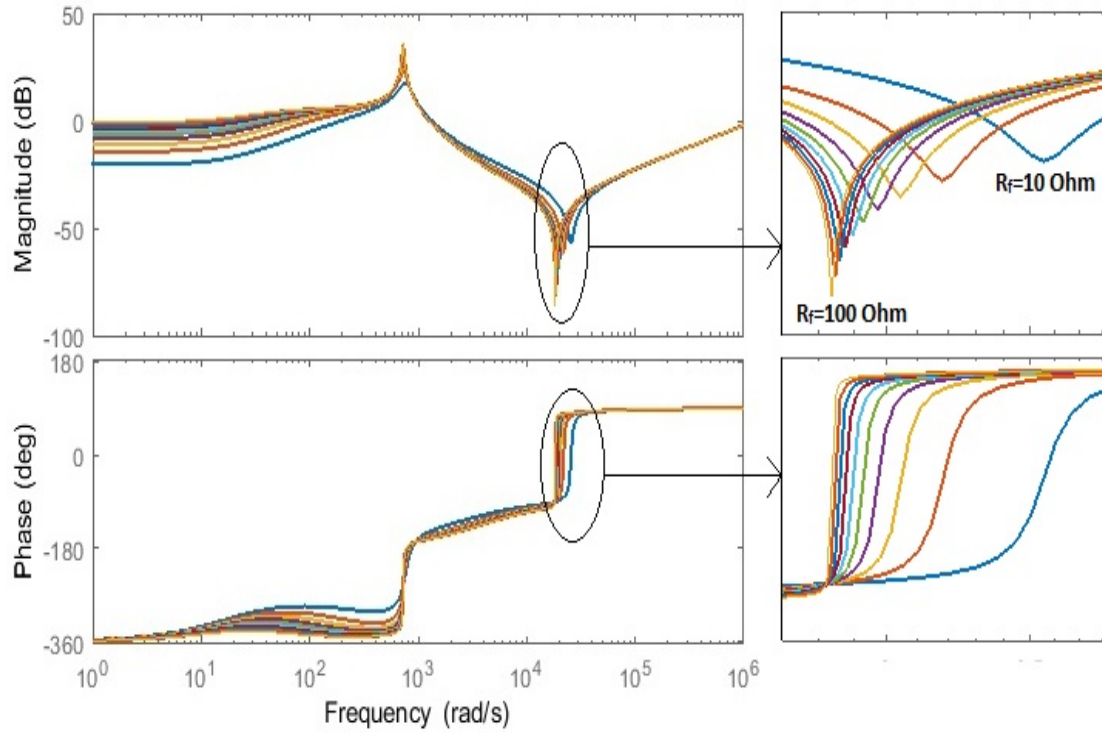


Figure 4.26: Frequency Response of Type-V L-C-L Filter

Type-V filter response has two resonance frequency. The first resonance creates high voltage distortion, while second resonance point gives rise to current distortion. If converter generates harmonics equal to this resonance, then there will be high voltage distortion and current distortion. However, with lower value of resistance, damping can be achieved. An additional inductor L_f can reduce the resistive loss.

4.8.2 Active Damping of Filter

Grid connected converters may not function stably under the harmonic resonance condition. Harmonic resonance occurs when the converter impedance and grid impedance becomes equal in magnitude and 180° out of phase. The converter is generally connected to grid through filters, which is mostly L-C-L type. So, the parameters of L-C-L filters

behaviour and good output voltage. The feedback of current is taken from branch between the two capacitors. First capacitor has value of βC and the second capacitor has value of $(1 - \beta)C$. Thus, the overall value of capacitor is C . The output impedance of system after adding virtual branch G_V is derived here.

$$((((V_{ref} - V_o)G_U - I_f)G_I - I_f G_V)K_{PWM} - V_o)\frac{1}{(Ls + r)} - V_o\beta Cs - I_o)\frac{1}{(1 - \beta)Cs} = V_o \quad (4.37)$$

Over a period, the average value of V_{ref} is equal to V_o . Also, the value of I_f is equal to $V_o(1 - \beta)Cs$. Putting this in equation (4.37) and then simplifying further gives.

$$\begin{aligned} V_o(-G_U G_I K_{PWM} + (1 - \beta)Cs G_I K_{PWM} + (1 - \beta)Cs G_V K_{PWM} \\ + \beta Cs(Ls + r) + (1 - \beta)Cs(Ls + r) = -I_o(Ls + r) \end{aligned} \quad (4.38)$$

$$V_o(-G_U G_I K_{PWM} + (1 - \beta)Cs K_{PWM}(G_V + G_I) + Cs(Ls + r)) = -I_o(Ls + r) \quad (4.39)$$

$$Z_o = \frac{V_o}{(-I_o)} = \frac{(Ls + r)}{(-G_U G_I K_{PWM} + (1 - \beta)Cs K_{PWM}(G_V + G_I) + Cs(Ls + r))} \quad (4.40)$$

If, $(1 - \beta)Cs K_{PWM}(G_V + G_I)$ is made equal to $G_U G_I K_{PWM}$, then

$$(1 - \beta)Cs K_{PWM}(G_V + G_I) = G_U G_I K_{PWM} \quad (4.41)$$

$$(G_V + G_I) = \frac{G_U G_I K_{PWM}}{(1 - \beta)Cs K_{PWM}} \quad (4.42)$$

Putting equation (4.42) in to (4.40),

$$Z_o = \frac{V_o}{(-I_o)} = \frac{(Ls + r)}{Cs(Ls + r)} \quad (4.43)$$

$$Z_o = \frac{V_o}{(-I_o)} = \frac{1}{Cs} \quad (4.44)$$

With the proper selected value of G_V , as shown above, the output impedance becomes capacitive. So, by selection of proper control loop and control parameter, the shaping of inverter output impedance can be effectively done. Also, the desired value of damping can be achieved. This method is known as active damping method. Like this, inverter can be made either L-Type or R-Type.

4.8.3 System Parameter for Converter Analysis

Table 4.1: System Parameter

Parameter	Value
Switching Frequency	4 KHz
Switching Delay	20 μ S
L_c	4 mH
L_g	0.4 mH
C_f	5 μ F
k_p	1.2
k_i	11.6

4.9 Conclusion

The characteristics and response of impedance of grid connected inverter depends on the various factors like selection of output filter, filter's parameter, controller type, controller's parameter, structure of PLL, and the delay in switching of converter. In this chapter, using first order PI controller and different types of filter, it is tried to explain in a simple way. The complexity of impedance increases with the order of the controller and its structure. Also, the reshaping of inverter impedance can be done by selection of suitable control structure. By adding virtual impedance the output impedance can be made inductive, capacitive or reactive without adding any additional hardware. In this work, different variants of passive filters are explained and how their output impedance behaves at different frequency is also explained with the use of Bode plot. The active damping

method is explained, whereby damping is achieved without using resistor in the filter, which is considered as a very energy efficient method of achieving damping. The output impedance can be reshaped either by external hardware in the form of filter or by adding virtual control loop in the controller. The stability of converter depends on how converter output impedance interacts with the grid impedance. Numerous efforts have been made and can be found in literatures to achieve the stability only by reshaping the impedance. However, the stability region can be expanded by reshaping of impedance up to certain extent only. Only reshaping of impedance doesn't guarantee the converter stability with changing grid condition. Also, converter is more likely to fall in an unstable region with weak grid condition, but reshaping of impedance helps to prevent converter based generation from going unstable. By analysing the output impedance in the frequency domain, the controller parameters can be adjusted to reshape the output impedance. By increasing the proportional gain of the *PI* controller, the magnitude of the output impedance can be increased and can enhance the ability of harmonic rejection. By increasing the integral gain of the *PI* controller, the phase of the output impedance can be increased to improve the stability of system [350], [351].